

Comparative Studies on Combustion of Peanut and Tamarind Shells in a Bubbling Fluidized Bed: Fluidization Characteristics of Binary Alumina–Biomass Mixtures

Poramet Arromdee, Vladimir I. Kuprianov*, Chalisa Aunsakul, Chanisara Polthai,
Dusadee Tuenudomseel, Phongpeera Tangphong, Wanboon Sookkasem

School of Manufacturing Systems and Mechanical Engineering, Sirindhorn International Institute of Technology,
Thammasat University, Pathum Thani 12121, Thailand

*Corresponding Author. E-mail: ivlaanov@siit.tu.ac.th; Tel: (+662) 986 9009, ext. 2208; Fax: (+662) 986 9112

Abstract

Hydrodynamic regimes and characteristics of a gas–solid bed were experimentally studied in the conical section of a bubbling fluidized-bed combustor (FBC). Prior to tests, alumina sand of 0.3–0.5 mm particle sizes used as the inert bed material in the FBC was premixed with shredded peanut/tamarind shells in different mass fractions (MF): 0%, 2.5%, 5%, 7.5% and 10% (by wt.). Ambient air used as the fluidizing agent was injected into the conical alumina–biomass bed through a 13-bubble-cap air distributor. For each biomass fraction in the binary mixture, the pressure drop across the bed (Δp) was measured versus superficial velocity at the distributor exit (u) for three static bed heights (BH): 20 cm, 30 cm and 40 cm. The Δp - u diagrams were plotted for variable MF and BH and compared between the two biomass fuel options. Three sequent hydrodynamic regimes of the bed were found to occur in all test runs when increasing u from 0 to 4–5 m/s. With higher MF, main hydrodynamic characteristics of the bed – the minimum fluidization velocity (u_{mf}) and corresponding pressure drop (Δp_{mf}) – were found to be increased. The bed height showed apparent effects on these hydrodynamic characteristics, particularly on Δp_{mf} , for any arbitrary MF. Static bed heights of 30 cm seem to be an optimal range as ensuring stable fluidization of alumina–biomass mixtures and reasonable values of u_{mf} and Δp_{mf} . For the two biomass fuels, dimensionless dependencies of $\Delta p/\Delta p_{mf}$ on u/u_{mf} showed a similarity when ranging MF at fixed BH.

Keywords: Bubbling fluidized bed; Binary mixtures; Hydrodynamic regimes and characteristics.

1. Introduction

During the past few decades, fluidized-bed combustion systems have been increasingly used for direct conversion of biomass fuels into energy [1]. In such systems, the fluidized bed consists of fuel, char and ash particles, basically of irregular shape and variable size, mixed in a relatively small proportion with inert bed material

(typically, silica sand) used to facilitate effective mixing between solids and gases (combustion products) and thus to ensure stable ignition and combustion of fuel particles in the bed.

Hydrodynamic characteristics of a gas–solid bed are key input parameters for optimal design and operation of a fluidized-bed combustion system (furnace or combustor), as



well as for proper selection of auxiliary equipments. A large number of research studies have addressed hydrodynamic regimes and characteristics of columnar (cylindrical or prismatic) bubbling fluidized beds using a single bed material [2,3]. As shown in these studies, one of the major hydrodynamic characteristics of a fluidized bed – the minimum fluidization velocity (u_{mf}) – is essentially the function of the bed density, particle size and voidage, while a corresponding pressure drop across the bed (Δp_{mf}) is mainly dependent on weight as well as cross-sectional area of the bed. However, experimental studies revealed that for a fluidized bed using a binary mixture of silica/alumina sand and biomass, the u_{mf} exhibits a general trend to increase (compared to that for pure sand) with increasing the proportion of biomass in the mixture [4–6].

This work is generally aimed at studying a feasibility of utilization of some unconventional Thai biomass fuels via their direct combustion in a newly constructed bubbling fluidized-bed combustor with a cone-shaped bed (referred to as 'conical FBC') using alumina sand as the inert bed material in order to prevent the bed agglomeration and possible defluidization [1,6]. Pioneering studies have reported the reliable operation of the pilot conical FBC (using silica sand as the inert bed material), which exhibited high combustion efficiency and acceptable emission characteristics for firing conventional Thai biomass fuels, such as rice husk, woody sawdust and pre-dried sugar cane bagasse [7]. Unlike columnar reactors with similar heat input, a conical FBC employs a lesser amount of the

inert bed material, which may result in saving auxiliary fuel during the combustor start up.

However, some related research studies have reported a substantial difference in the behavior of conical and columnar fluidized beds with identical bed materials and geometry [8–10]. In particular, these studies revealed the partially fluidized-bed regime of a conical gas–solid bed through which the bed undergoes a transition from the fixed-bed state to the fully fluidized-bed regime. Substantial effects of (i) bed particle size, (ii) static bed height and (iii) bed cone angle on u_{mf} and Δp_{mf} , as well as on the relationship between the pressure drop across a conical bed (Δp) and the fluid superficial velocity at the bed bottom plane (u) (generally termed the Δp - u diagram), have also been reported in these studies.

As can be concluded from the literature review, there is a lack of data on hydrodynamic regimes and characteristics of binary mixtures fluidized in a bubbling conical bed, which would affect the bed behavior, as well as the range of operating conditions, particularly of (primary) air supplied to the biomass-fuelled combustor.

The main objective of this cold-state study was to examine the behavior of two types of binary mixtures – (1) alumina sand and shredded peanut shells, and (2) alumina sand and shredded tamarind shells – fluidized in a conical bed by ambient air with the aim to determine the effects of the shell mass fraction in the mixture and also static bed height on the major hydrodynamic characteristics, as well as on the entire Δp - u diagram, of the conical gas–solid beds with selected materials.

2. Methodology

2.1 Experimental facilities

Fig. 1 shows the schematic diagram of the conical FBC designed and constructed for firing Thai unconventional biomass fuels, including peanut and tamarind shells. To avoid the risk of bed agglomeration (defluidization), alumina was selected to be the inert bed materials in this combustor for firing peanut/tamarind shells with their elevated alkali contents. The combustor consisted of two main sections: (1) a conical section with a 40° cone angle and 0.25 m inner diameter at the bottom base, and (2) a cylindrical one with 2.5 m height and 0.9 m inner diameter. As the conical FBC was primarily designed for biomass combustion, the reactor was equipped with facilities for fuel supply (a fuel feeder) and pre-heating of the bed material (a start-up burner), both being out of operation in these cold-state experiments for the bed hydrodynamics. Air was injected into the

bed at the combustor bottom plane through the air distributor generating a fluidized bed in the conical section.

All cold-state trials were performed on the conical part of the combustor. Fig. 2 depicts the experimental set-up for these trials. As seen in Fig. 2a, the experimental facilities included the conical FBC filled with the bed material (alumina sand or alumina-biomass mixture) at the bottom section, and a 25-hp blower supplying ambient air (at about 30 °C) to the combustor through an air pipe of 0.1 m inner diameter (Fig. 2a). The airflow rate was controlled by a butterfly valve located downstream from the blower.

A relationship between the airflow rate (Q_a) (quantified by integrating the velocity profile across the air pipe and the valve opening) was determined prior to the main experimental tests. A multifunction flowmeter “Testo-512” (Testo AG, Germany) with the L-type Pitot tube was used to measure air velocity across the pipe in calibration tests. With this method, the measurement accuracy of the airflow rate was ensured at ± 0.03 m/s, when ranging the air velocity from 0 to 10 m/s. However, due to errors in physical measurement of a pipe inner diameter ($\pm 1\%$) and uncertainty in the velocity profile ($\pm 2\%$), the measurement uncertainty in the airflow rate was estimated to be $\pm 3\%$.

The bubble-cap air distributor used in this conical FBC was made up of thirteen stand pipes fixed on the distributor plate (Fig. 2b). An individual stand pipe had 64 holes (nozzles) each of 2 mm in diameter, distributed evenly over the pipe surface, and also four vertical slots with the flow area of 180 mm² (total) located under the caps of 46 mm diameter. Thus, the

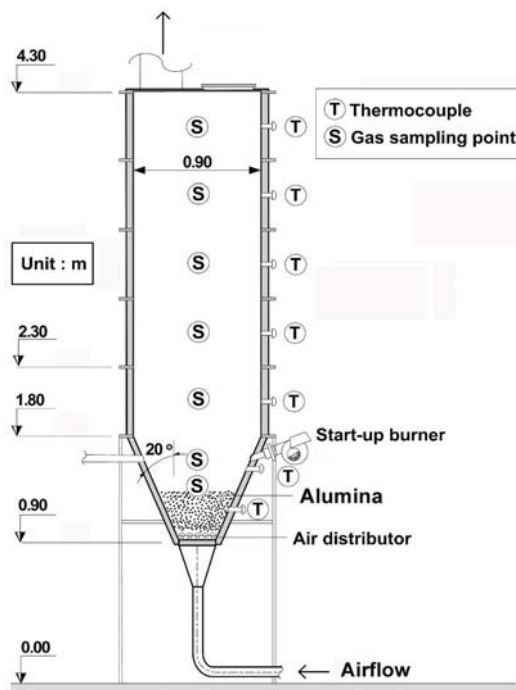


Fig. 1. Schematic diagram of the conical FBC.

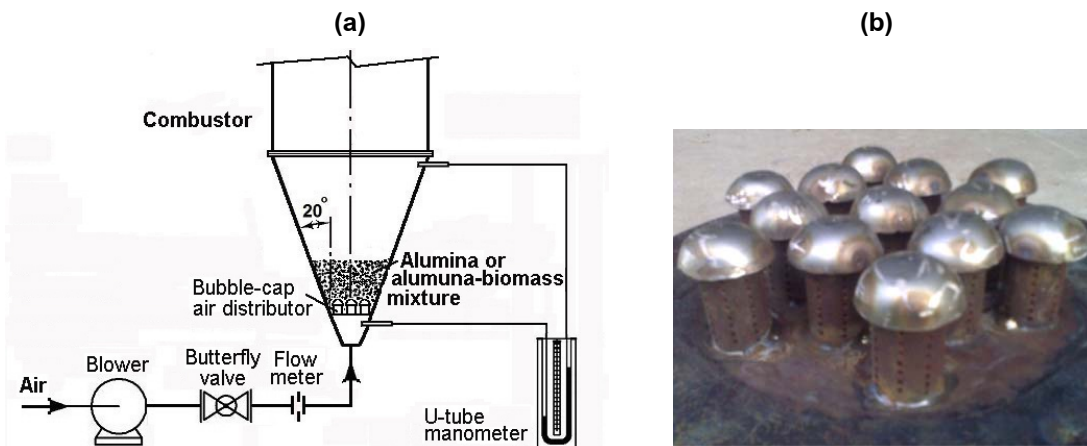


Fig. 2. (a) Experimental set-up for the cold-state hydrodynamic study on the conical FBC and (b) bubble-cap air distributor with thirteen stand pipes used to generate the bubbling fluidized bed.

net cross-sectional area of airflow at the distributor exit (calculated as difference between the area of the 0.25-m-diameter distributor plate and total area occupied by the stand pipe caps) was $A_a = 0.027 \text{ m}^2$. Hence, for the particular operating conditions, the superficial air velocity related to the bottom bed plane was estimated as $u = Q_a/A_a$ with the uncertainty of $\pm 3\%$.

2.2 Procedures

Alumina sand ($\text{Al}_2\text{O}_3 = 94.4\%$, $\text{SiO}_2 = 3.5\%$, $\text{TiO}_2 = 2.74\%$, and some other oxides) with a solid density of about 3400 kg/m^3 and sieve particle sizes of 0.3–0.5 mm was prepared for the experiments.

As it was planned for the combustion tests, peanut and tamarind shells were used as shredded fuels to ensure smooth fuel feeding to the combustor and also to improve hydrodynamic characteristics of the fluidized bed. Both shredded shells exhibited irregular shape and variable size of particles – from fine sawdust-like particles to flake-shaped particles with the maximum sieve size of approximately 5 mm. To meet the work objectives, alumina sand was

premixed with shredded peanut/tamarind shells in different biomass fractions or percentages (MF) in the binary mixture: 0% (i.e., using pure alumina), 2.5%, 5%, 7.5% and 10% (all by wt.).

Prior to trials, alumina sand or a binary alumina–biomass mixture was placed in the conical section forming a loosely packed bed. For each selected MF, the static bed height (BH) was variable: 20 cm, 30 cm and 40 cm. To measure the total pressure drop across the bed and air distributor, Δp , one of the two static pressure probes connected to the U-tube manometer was allocated in the air duct below the air distributor, while the second one was fixed at the top of the conical section of the combustor, as shown in Fig. 2a.

The uncertainty in pressure drop (Δp) of $\pm 2\%$ was basically affected by the correctness of fixation of the static pressure tubes in the airflow, as well as by the error in reading of the U-tube manometer. For the selected MF and BH, the pressure drop across the bed was measured versus the superficial velocity to provide data for plotting the Δp - u diagram, which

afterwards was used to determine the major

3. Results and Discussion

3.1 Flow regimes of an air–alumina bed

Fig. 3 shows the Δp - u diagram of the conical bed for three selected BHs when using pure alumina as the bed material (solid dots) and the contribution of the pressure drop across the air distributor to the total Δp for variable u (open dots). It can be seen in Fig. 3 that for each BH the air–alumina bed exhibited three sequent flow regimes when varying u from 0 to 4–5 m/s: (1) the fixed-bed regime, (2) the partially fluidized-bed (PFB) regime, and (3) the fully bubbling fluidized-bed (BFB) regime, like those found in conical beds with similar geometry using silica sand [10].

Within the fixed-bed regime ($u < u_{mf}$), Δp gradually increased with higher u , until its value attained Δp_{mf} at $u = u_{mf}$. With increasing BH, the minimum fluidization velocity of alumina particles with the selected sieve size (0.3–0.5 mm) showed the trend to be increased: from $u_{mf} = 0.26$ m/s at BH = 20 cm to $u_{mf} = 0.54$ m/s at BH = 40 cm, mainly due to the greater bed weight. This effect (typical for conical gas–solid beds [9,10]) resulted in an increase of corresponding (total) pressure drop that occurred

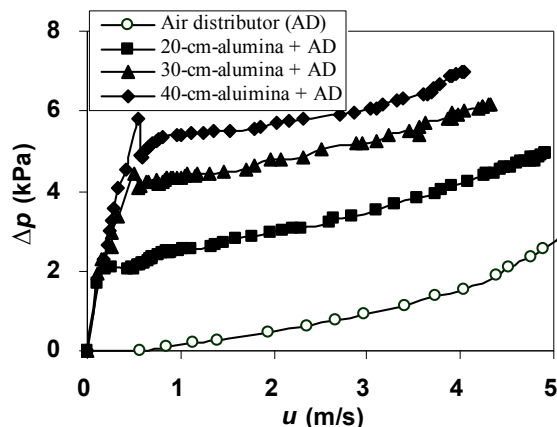


Fig. 3. The Δp - u diagrams of a conical alumina bed for different bed heights and air distributor.

hydrodynamic characteristics for each trial.

at $u = u_{mf}$: from $\Delta p_{mf} = 2.1$ kPa at BH = 20 cm to $\Delta p_{mf} = 5.8$ kPa at BH = 40 cm. During the PFB regime, Δp abruptly reduced (roughly by 15–20%, i.e., by a substantially greater value than in columnar beds at similar BHs), when u was increased from u_{mf} to the value termed the minimum velocity of full fluidization (u_{mff}), the latter being quite close to u_{mf} . Within the BFB regime ($u \geq u_{mff}$), due to effects of the pressure drop across the air distributor, Δp was found to be increased with higher u (at nearly the same rate for all BHs). If the pressure drop across the air distributor were subtracted from Δp , the pressure drop across the fluidized bed would be represented for $u \geq u_{mff}$ by an invariant characteristic, confirming the occurrence of bubbling fluidization regime in the beds with selected geometrical characteristics and material properties.

3.2 Hydrodynamics of alumina–biomass beds

Fig. 4 compares the Δp - u diagrams of the conical beds with selected BHs using alumina sand mixed with shredded peanut shells between the test runs for variable biomass fraction in the binary mixture (MF). Like for the beds with pure alumina, the Δp - u diagrams of the beds with binary mixtures exhibited the above-mentioned regimes, however, with some apparent effects from the biomass.

Within the fixed-bed regime, the gradient $d(\Delta p)/du$ in all the tests was not as smooth as for the case of pure alumina beds, particularly, at superficial velocities of 0.2–0.5 m/s (see Fig. 4). At fixed BH, u_{mf} showed a substantial increase (at rate depending on BH) when ranging MF from 0 (for pure alumina bed) to 5

wt.%, because of the influence of coarse biomass particles. However, with further increasing MF (from 5 wt.% to 10 wt.%), u_{mf} stayed constant, which is unusual for columnar beds [5,11]. It can be seen in Fig. 4 that in all the trials with mixtures, u_{mf} was characterized by reasonable values: from about 0.5 m/s to 0.8 m/s (maximum). Compared to data for the alumina sand beds (see Fig. 3), Δp_{mf} for the binary mixtures increased insignificantly, by maximum 1 kPa, for the selected BH and MF. Responding to the behavior of u_{mf} , Δp_{mf} exhibited similar effects of MF for all BHs. Note that the difference between u_{mff} and u_{mf}

(associated with the occurrence of PFB regime) noticeably increased with greater MF. Furthermore, this effect was stronger for higher beds. For instance, at MF = 10 wt.% and BH = 40 cm, the value of u_{mff} was rather high, about 1.5 m/s. For the expected proportion of biomass in the binary mixture of less than 5% [5,6], both u_{mf} and u_{mff} were found to be at an acceptable level (below 0.8 m/s) for the 20–30 cm beds, and Δp did not exceed 5 kPa. As for the BFB regime, an apparent influence of the pressure drop across the air distributor on the Δp - u diagram was observed in all trials, especially, at higher superficial velocities. For the 20-cm static

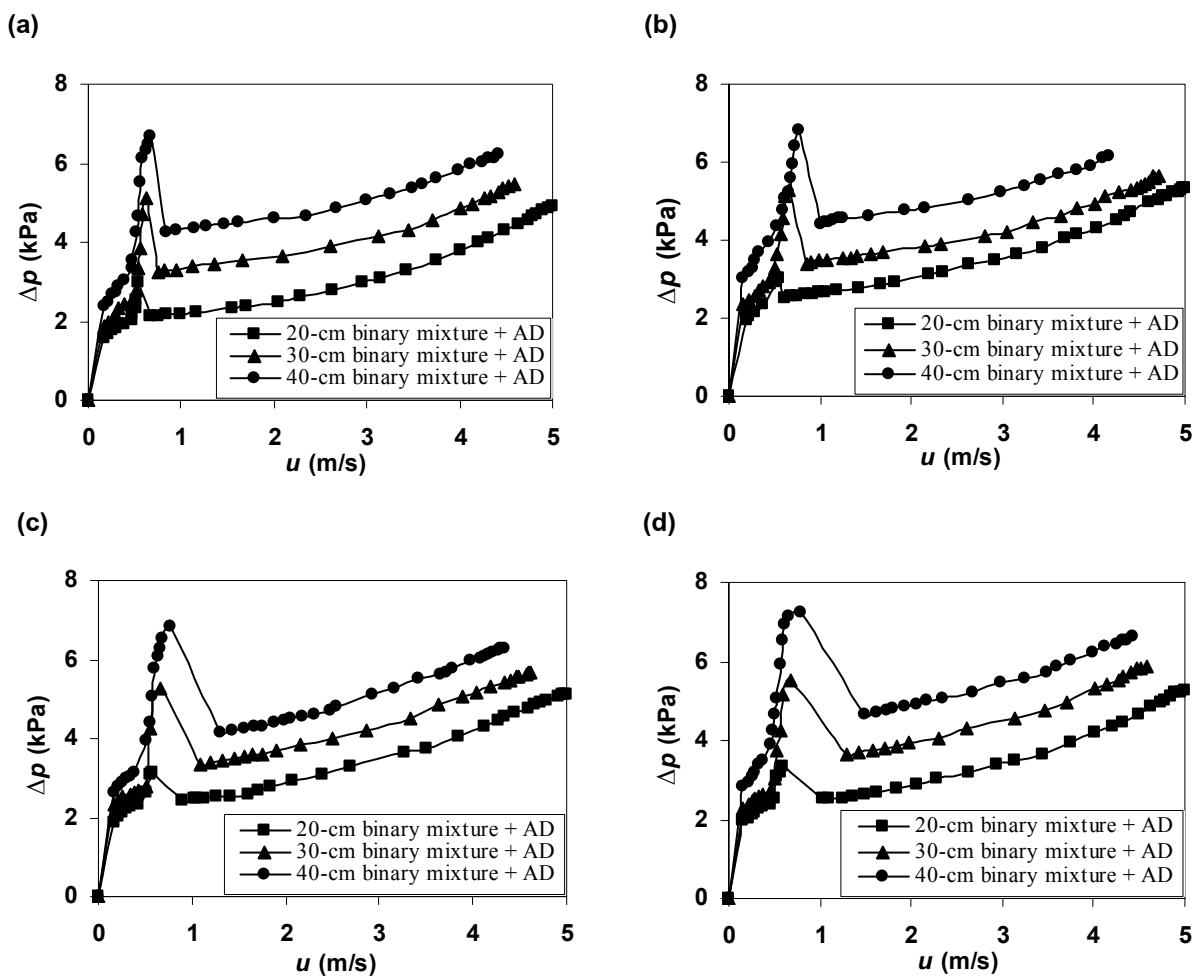


Fig. 4. Effects of static bed height on the Δp - u diagram of alumina mixed with shredded peanut shells for variable wt.% of biomass in the mixture: (a) 2.5 wt.%, (b) 5.0 wt.%, (c) 7.5 wt.% and (d) 10 wt.%.

bed height, Δp - u dependences for the fully fluidized beds in different trials were represented by quite similar profiles (regardless of MF). However, at any arbitrary u within the BFB regime, the Δp values for binary mixtures at BH = 30 cm and BH = 40 cm were noticeably lower than those for alumina beds, mainly due to the lowering of the bed density, which made the abrupt reduction of Δp during the PFB regime of the mixtures to be more significant than for the pure alumina beds. In the meantime, as can be seen in Fig. 4, the effects of MF on the behavior of Δp at $u \geq u_{\text{mf}}$ were rather weak.

Fig. 5 depicts the Δp - u diagrams of the

conical beds of alumina sand mixed with tamarind peanut shells for the same operating conditions, as in Fig. 4. As compared between the results in Fig. 5 with those in Fig. 4 at similar MF, the Δp - u diagrams of the beds with tamarind shells were quite similar to those of the beds with peanut shells, showing that the bed behavior was independent of MF but affected by BH and pressure drop across the air distributor. However, when using shredded tamarind shells with (almost) no fibers, the behavior of Δp in the fixed-bed regime was represented by parabolic-like smooth-gradient curves (typical for conical air-sand beds [10]) for all the trials. For the

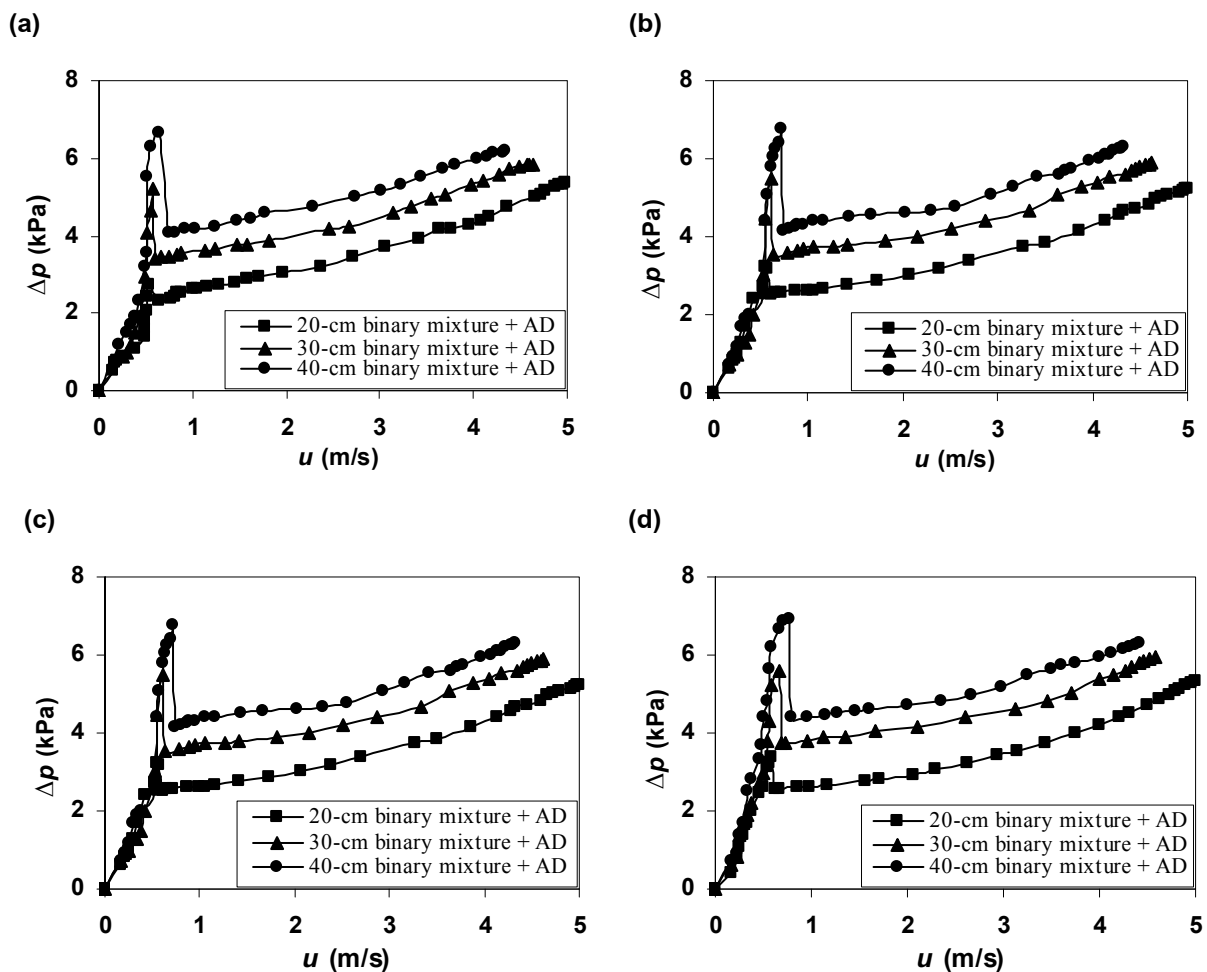


Fig. 5. Effects of the static bed height on the Δp - u diagram of alumina mixed with shredded tamarind shells for wt.% of biomass in the mixture: (a) 2.5 wt.%, (b) 5.0 wt.%, (c) 7.5 wt.%, and (d) 10 wt.%.

binary mixtures with these shells, both u_{mf} and Δp_{mf} were almost independent of MF. The values of u_{mf} were found to be close to u_{mf} for given operating conditions, and the beds with binary mixtures apparently exhibited the same features as the fluidized beds with pure alumina.

It can be generally concluded that within the BFB, the Δp - u dependencies for both types of the binary mixtures were quite similar for different MFs (at fixed BH) and showed similar effects of BH. However, the static bed height of 30 cm seems to be an optimal value as ensuring stable fluidization of the gas–solid bed at reasonable u_{mf} and Δp_{mf} .

3.3 Relative hydrodynamic characteristics

Fig. 6 compares the dependencies of the relative total pressure drop across the air distributor and alumina–biomass bed ($\Delta p/\Delta p_{mf}$) on the relative superficial velocity (u/u_{mf}) for variable MF of peanut/tamarind shells in the binary mixture between two static bed heights: BH = 20 cm and 30 cm. For each BH, the dependence $\Delta p/\Delta p_{mf} = f(u/u_{mf})$ obtained via treatment of experimental data for given biomass

showed an apparent similarity for different test runs. Furthermore, at fixed BH, the values of $\Delta p/\Delta p_{mf}$ for the two biomass fuels were quite close at any arbitrary u/u_{mf} ranged from 1.5 to 3, exhibiting an apparent divergence with further increasing of u/u_{mf} . Note that the dimensionless dependencies $\Delta p/\Delta p_{mf} = f(u/u_{mf})$ for the beds at BH = 40 cm using peanut/tamarind shells looked quite similar to those for 30-cm bed height, especially in the fixed-bed region, with $\Delta p/\Delta p_{mf}$ being slightly lower during BFB regime at similar conditions. In the meantime, with increasing BH, the relative reduction in the total pressure drop during the PFB regime became more significant, while the gradient $d(\Delta p/\Delta p_{mf})/d(u/u_{mf})$ during the BFB regime exhibited some reduction, mainly due to the lower relative contribution of the pressure drop across the air distributor to Δp . Thus, in the case of using shallow beds (≤ 30 cm), the air distributor needs some modification leading to reduction of the elevated pressure drop across the air distributor, especially at higher u/u_{mf} , and thus enabling to select the blower with lesser consumption of energy.

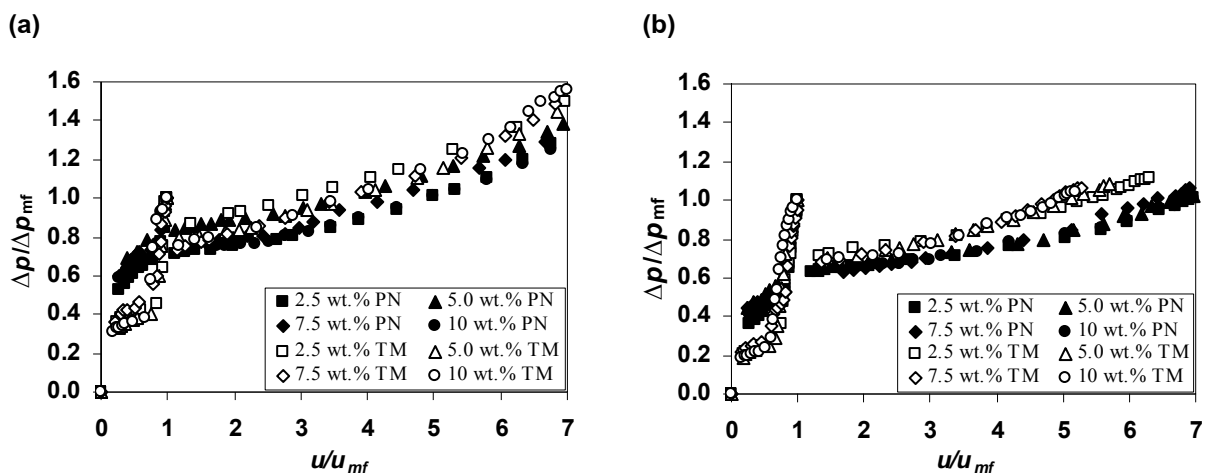


Fig. 6. Relative pressure drop (across the bed–distributor) versus relative superficial velocity for variable wt.% of peanut (PN) and tamarind (TM) shells mixed with alumina at (a) BH = 20 cm and (b) BH = 30 cm.

3.4 Impact of hydrodynamic characteristics on operating regime of the conical FBC

The conical FBC shown in Fig. 1 was designed to burn 60 kg/h of peanut/tamarind shells at the specified range of excess air of 20–80% [12]. Note that both fuels had quite similar lower heating value (of about 16 MJ/kg) and therefore required similar amount of stoichiometric air (of about 4.7 Nm³/kg). Hence, it can be estimated (using the stoichiometric volume of air) that to ensure the specified fuel feed rate, the superficial air velocity at the bottom plane of the conical bed should be maintained in the range from 4.2 m/s to 6.2 m/s (when increasing excess air from 20% to 80%) for the two fuels.

Using the results from this cold-state studies at reasonable percentages of biomass in the binary mixture (2.5–5 wt.%) and selected static bed height (BH = 30 cm), u_{mf} for the two fuel options can be roughly estimated by a single value (about 0.7 m/s). So, in the tests for firing the fuels in this combustor, u can be maintained within $(6-9)u_{mf}$ for the ranges of operating conditions. Thus, the conical FBC was expected to ensure the bubbling fluidization regime in all combustion tests.

4. Conclusions

Hydrodynamic regimes and characteristics of a cone-shape air–solid bed with variable, 20–40 cm, static bed height (BH) have been experimentally studied under cold-state conditions in the conical section of a fluidized-bed combustor with a 40° cone angle designed and constructed for firing peanut/tamarind shells and other unconventional biomass fuels. The behavior and characteristics of fluidization of the bed have been studied

using alumina sand as the inert bed material mixed with shredded peanut/tamarind shells in variable biomass fraction (MF) in the mixture (from 0 to 10 wt.%).

The specific conclusions from this research study are as follows:

(1) Three sequent hydrodynamic regimes (fixed-bed, partially fluidized-bed, and fully bubbling fluidized-bed regimes) are observed in the conical fluidized bed when varying the air superficial velocity from 0 to 4–5 m/s for the selected ranges of BH and MF.

(2) With increasing BH, the major hydrodynamic characteristics of an alumina (or alumina–biomass) bed, the minimum fluidization velocity (u_{mf}) and corresponding total pressure drop across the air distributor and fluidized bed (Δp_{mf}), show the trend to be increased. For the beds with alumina–biomass mixtures at 20–30 cm MHs and typical MFs (less than 5%), u_{mf} is at an acceptable level (below 0.8 m/s), while Δp_{mf} does not exceed 5 kPa.

(3) Within the partially fluidization regime, the total pressure drop (across the air distributor and fluidized bed) reduces abruptly (by 20–40%, depending mainly on BH) while the air superficial velocity (u) at the air distributor exit is increased from u_{mf} to the minimum velocity of the fully fluidized-bed regime (u_{mff}). For the binary mixtures with peanut shells, the difference between u_{mff} and u_{mf} is noticeable and apparently affected by both BH and MF; however, this difference is rather small for the mixtures with tamarind shells.

(4) Within the bubbling fluidized-bed regime, the Δp - u dependencies for the two types of binary mixtures are quite close for different MFs (at



fixed BH) and show similar effects of BH. For fixed BH, the dependence $\Delta p/\Delta p_{mf} = f(u/u_{mf})$ for this regime exhibit an apparent similarity for the test runs with different types of binary mixtures for the range of MF.

(5) The static bed height of 30 cm seems to be an optimal value as ensuring stable fluidization of the gas–solid bed at reasonable u_{mf} and Δp_{mf} .

5. Acknowledgements

The authors would like to acknowledge the financial support from the Thailand Research Fund and Thammasat University (Contract No. BRG 5380015), and from the Commission on Higher Education, Ministry of Education, Thailand (Contract No. 6/2551).

6. References

- [1] Khan, A.A., de Jong, W., Jansens, P.L. and Spliethoff, H. (2009). Biomass combustion in fluidized bed boilers: Potential problems and remedies, *Fuel Processing Technology*, vol. 90, pp. 21–50.
- [2] Geldart, D. (1973). Types of gas fluidization, *Powder Technology*, vol. 7, pp. 285–292.
- [3] Kunii, D. and Levenspiel, O. (1991). Fluidization Engineering, *Butterworth-Heinemann*, Boston.
- [4] Pilar Aznar, M.P., Gracia-Gorria, F.A. and Corella J. (1992). Minimum and maximum velocities for fluidization for mixtures of agricultural and forest residues with a second fluidized solid: II. Experimental results for different mixtures, *International Chemical Engineering*, vol. 32, pp. 103–113, 1992.
- [5] Rao, T.R. and Ram Bheemarasetti, J.V. (2001). Minimum fluidization velocities of mixtures of biomass and sands, *Energy*, vol. 26, pp. 633–644.
- [6] Sun, Z., Jin, B., Zhang, M., Liu, R. and Zhang, Y. (2008). Experimental study on cotton stalk combustion in a circulating fluidized bed, *Applied Energy*, vol. 85, pp. 1027–1040.
- [7] Permchart, W. and Kouprianov, V.I. (2004). Emission performance and combustion efficiency of a conical fluidized-bed combustor firing various biomass fuels, *Bioresource Technology*, vol. 92, pp. 83–91.
- [8] Peng, Y. and Fan, L.T. (1997). Hydrodynamic characteristics of fluidization in liquid-solid tapered beds, *Chemical Engineering Science*, vol. 52, pp. 2277–2290.
- [9] Jing, S. Hu, Q. Wang, J. and Jin, Y. (2000). Fluidization of coarse particles in gas–solid conical beds, *Chemical Engineering and Processing*, vol. 39, pp.379–387.
- [10] Kaewklum, R.. and Kuprianov, V.I. (2008). Theoretical and experimental study on hydrodynamic characteristics of fluidization in air–sand conical beds. *Chemical Engineering Science*, vol. 63, pp. 1471–1479.
- [11] Zhang, Y., Jin, B. and Zhong, W. (2009). Experimental investigation on mixing and segregation behavior of biomass particles in a fluidized bed, *Chemical Engineering and Processing: Process Intensification*, vol. 48, pp. 745–754.
- [12] Arromdee, P., Kuprianov, V.I., Nithikan, M., Wongjaturapat, N., Pasutnavin, R., Tilokkul, T., Thamrongdullapark, V. and Lamlertpongpana, W. (2011). Comparative studies on combustion of peanut and tamarind shells in a bubbling fluidized bed: Combustion and Emission Characteristics. In *Proceedings of The Second TSME Conference on Mechanical Engineering*, 19–21 October, 2011 (in this volume).